ELEMENTAL PARTITIONING CONSTRAINTS ON THE MINERALOGY OF THE MARTIAN MANTLE. S. Yang[1], M. Humayun[1], K. Righter[2], A. J. Irving[3], R. H. Hewins[4,5] and B. Zanda[4,6]. [1]Florida State University, Tallahassee, FL 32310, USA (syang@magnet.fsu.edu); [2]NASA Johnson Space Center, Mail code XI2, Houston, TX 77058, USA; [3]Department of Earth and Space Sciences, University of Washington, Seattle, WA 98195, USA; [4]IMPMC, Sorbonne Université, MNHN-UPMC, 75005 Paris, France; [5]Rutgers University, Piscataway, NJ 08854, USA; [6]IMCCE, Observatoire de Paris - CNRS UMR 8028, 75014 Paris, France.

Introduction: Incompatible elements weakly partition into mantle mineral phases so precise measurements of incompatible element abundances in mantle melts have been used to infer mineralogy of mantle sources [1, 2]. In a recent study [3], we showed that several incompatible chalcophile elements (As, Tl, Pb) relative to REE were more compatible in martian igneous rocks than in terrestrial basalts. This observation can be accounted for by (1) the bulk partition coefficients of chalcophile elements being higher due to the presence of more residual sulfide in the martian mantle [3] and/or (2) different relative compatibilities in the martian mantle due to differences in mineralogy. In this study, the compatibility sequences of lithophile elements in martian and MORB mantles are revised to better represent relative partitioning behavior during mantle differentiation and the influence of mantle mineralogy is examined.

Methodology: On a logarithmic concentration plot, a pair of elements with identical partition coefficients yields a correlation with a slope of unity [1]. A slope above unity indicates the element on the y-axis is less compatible than the element on the x- axis and *vice versa*. The relative compatibilities of incompatible trace elements in martian meteorites were assessed using data from this study and from literature sources. Fig. 1 provides an example where the relative compatibility of Th, U, Nb and Ce were assessed against that of La for shergottites and for MORBs. The shergottite dataset used here includes new measurements by LA-ICP-MS [3, 4], solution ICP-MS [5], and from [6]. A global MORB dataset from [7] and an estimate of bulk silicate Mars [8] are plotted for comparison. The slopes of the correlations in Fig. 1 were calculated using York regression [9] where errors in both elemental concentrations were taken into account.

Results: Two important observations are made in Fig. 1: (1) the relative order of compatibility, Th < Nb < U < La < Ce, is the same in shergottites and in MORBs [1]; but, (2) the relative magnitude of compatibilities of Th, Nb and U against La in shergottites are more similar than that of MORBs as judged by the slopes of the correlations in Fig. 1. For example, the compatibilities of Th and Nb and that of U and La are nearly identical in shergottites whereas notable differences in compatibility are noted in MORBs for these elements. The slope of log [Th] vs. log [La] in shergottites is 1.18, compared to 1.65 in MORBs (Fig. 1a). The range of relative compatibilities of Th, Nb, U and Ce to La are smaller in shergottites than in MORB.

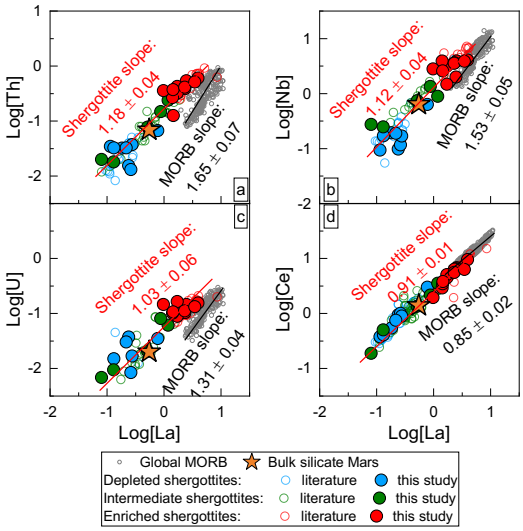

Fig. 1(a-d): Correlations of log concentration of La vs. that of Th, Nb, U and Ce for depleted, intermediate and enriched shergottites from this study and literatures [5, 6], MORBs [7], and bulk silicate Mars (BSM) [8].

A matrix of inter-element compatibility was constructed for all available lithophile trace elements varying from highly incompatible to moderately incompatible to construct the compatibility orders in shergottites and in MORBs. The result is summarized in Fig. 2 where elements are plotted according to their compatibility with respect to La taken as 1.0. Since this set of elements spans a broad range of compatibility, and reliable comparisons are best made against an element of similar compatibility, a boot-strap method was used to place the various REE relative to La and then other elements were arranged according to their slopes to the nearest REE of similar compatibility.

In Fig. 2, the bulk silicate Earth (BSE)-normalized composition of average N-MORB [7, 10] and BSM-normalized composition of Tissint [8, 11] are plotted on this new relative compatibility scale that takes the magnitude of the difference in compatibility into account. Interestingly, Fig. 2 shows that (1) the order of relative compatibility of the majority of lithophile trace elements is similar between Tissint and N-MORB, except K and P are significantly more compatible with

respect to other elements in Tissint than in N-MORB; (2) the highly incompatible elements are less incompatible relative to La in Tissint than in N-MORB; while (3) the HREEs are more compatible in Tissint than in N-MORB.

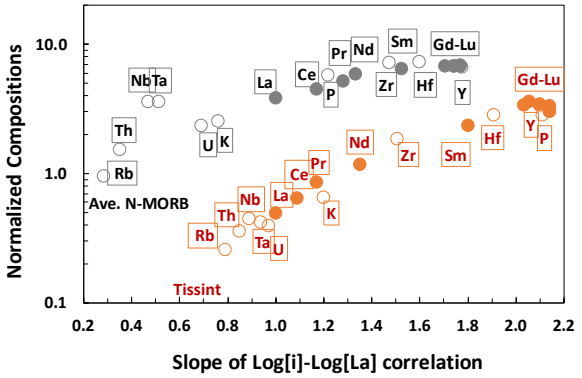

Fig. 2: Bulk silicate Mars (BSM) [8] normalized concentration of Tissint [11] and BSE [10] normalized concentration of average N-MORB [7].

Discussion: Previous modeling [e.g., 12, 13] and experimental [14] studies have shown that the partition coefficients of REEs between olivine, pyroxenes and shergottite magmas are similar to those for terrestrial basalts [14]. Thus, trace element partitioning will be determined by mantle mineralogy that could be constrained empirically by the variations of the relative compatibilities of trace elements (Fig. 2).

There are numerous determinations of the partition coefficients of incompatible trace elements between basaltic melt and mantle minerals, but there are few studies that have analyzed a broad range of elements within a single experiment. Variations from experiment to experiment are large, controlled by temperature, pressure, mineral and melt composition. To estimate the bulk partition coefficients of lithophile trace elements in the martian mantle, we used experimentally determined partition coefficients from [15] because these experiments were run at temperatures similar to that of shergottite partial melting (1500-1600 °C), and were multiply-saturated with pyroxenes and garnet. Noticeably, the differences of partition coefficients of trace elements between clinopyroxene (cpx) and orthopyroxene (opx) are small [15], as Ca contents converge between cpx and opx at these temperatures [16]. Thus, cpx and opx were combined as a single pyroxene phase in our calculation of bulk partition coefficients of martian mantle (Fig. 3). The partitioning of incompatible elements in olivine is negligible [17]. For the terrestrial mantle, the mineralogy of KLB-1 (ol: pyx: grt= 61: 30: 9) at 3 GPa [18] was used and for the martian mantle the mineralogy (ol: pyx: grt= 45: 45: 10) from [8] was used as a reference model. The modal proportions of olivine, pyroxene and garnet were then varied to ascertain the influences of each mineral on the partitioning. Fig. 3 shows the bulk D of a set of putative martian mineralogies normalized to KLB-1. The lower abundance of olivine in [8] makes the incompatible trace elements more compatible in the martian mantle relative to the terrestrial mantle. Models with higher ratios of garnet (15-20 %) to pyroxene capture the higher compatibility of the REE and explain the relatively more compatible nature of Th, Nb and U (Fig. 2). Improved partition coefficients for martian mantle compositions could better constrain mantle source mineralogy for shergottites. The effect of silicate mineralogy on partitioning of chalcophile (As, Pb, Tl) elements will need to be assessed.

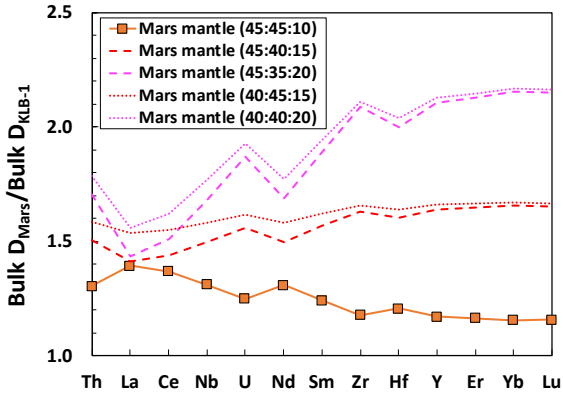

Fig. 3: Bulk partition coefficients (D) for modeled martian mantle mineralogies normalized to that of KLB-1 (terrestrial). Orange line with squares represents the mineralogy of BSM [8].

References: [1] Nielsen S. et al. (2014) *G³ 15*, 4905-4919. [2] Salters V. J. M. (1996) *EPSL 141*, 109-123. [3] Yang S. et al. (2020) LPSC LI *abstract #1300.* [4] Yang S. et al. (2015) *MaPS 50,* 694-714. [5] Day J. M. D. et al. (2018) *Nat. Commun. 9*, 1-8. [6] Meyer C. (2009) Martian Meteorites Compendium. [7] Yang S. et al. (2020) *Sci. Adv. 6,* eaba2923. [8] Yoshizaki T. and McDonough W. F. (2020) *GCA 273,* 137-162. [9] York D. et al. (2004) *Am. J. Phys. 72*, 367-375. [10] McDonough W. F. and Sun S.-S. (1995) *Chem. Geol.* 120, 223-253. [11] Aoudjehane H. C. et al. (2012) *Science 338,* 785-788. [12] Borg L. and Draper D. S. (2003) *MaPS 38,* 1713-1731. [13] Shimoda G. et al. (2005) *EPSL 235,* 469-479. [14] Blinova A. and Herd C. (2009) *GCA 73,* 3471-3492. [15] Salters V. J. M. and Longhi J. E. (1999) *EPSL 166*, 15-30. [16] Lindsley D. H. (1983) *Am. Min. 68,* 477-493. [17] Beattie P. et al. (1991) *Contrib. Mineral. Petrol. 109,* 212-224 [18] Davis F. et al. (2011) *EPSL 30*, 380-390.